Progress In Electromagnetics Research, PIER 83, 257–277, 2008

HYBRID EMPIRICAL-NEURAL MODEL OF LOADED MICROWAVE CYLINDRICAL CAVITY

Z. Stanković, B. Milovanović, and N. Dončov

Faculty of Electronic Engineering
University of Niš
Aleksandra Medvedeva 14, 18000 Niš, Serbia

Abstract—A hybrid empirical-neural (HEN) model, to account for a loading effect of arbitrary raised dielectric slab in a microwave cylindrical metallic cavity, is presented. It is based on combination of an approximate model, as a rough empirical knowledge holder, and multi-layer perceptrons (MLP) neural network. In comparison with the model based only on MLP network, more accurate and efficient resonant frequencies calculation is achieved.

1. INTRODUCTION

The cylindrical metallic cavities loaded by homogeneous dielectric slabs represent a configuration very suitable for good modeling of some practical microwave applicators used for thermal dielectric material processing in industry. The knowledge of the mode tuning behavior in a cavity under loading condition (i.e., physical and electrical parameters of the load) forms an integral part of the studies in microwave heating and it can considerable help in designing these applicators [1].

Transverse resonance method (TRM) [2] is a conventional approach for carrying a theoretical analysis of the partially loaded cylindrical metallic cavities. Representing a loaded cavity as a cascade connection of the equivalent transmission lines, characteristic equation for resonance frequency calculation can be derived from the transverse resonance condition. In a general case, this equation is complex transcendental and its solution requires an appropriate numerical technique and an efficient mode identification procedure [3]. Such complex mathematical calculations are hardware and time consuming representing a main disadvantage of TRM approach. In order to overcome this limitation and allow an easy process of mode identification and resonant frequency measuring, a numerically very

simple empirical procedure for approximate determination of the resonant frequencies in loaded microwave cylindrical cavities was presented in [4]. However, it was applicable only to the simplified case of dielectric slab placed at the bottom of the cavity.

Artificial neural networks represent an accurate and faster alternative to the polynomial and empirical models conventionally used in microwave area [5–11]. This is particularly true either in the cases when device physics is not fully understood but device output for specified input is known or in the cases of high-dimensional and highly non-linear problems modeling. Classical multilayer perceptrons (MLP) network [5, 12], as one of existing artificial neural networks, is often used for that purposes allowing for extraction of all functional dependences of the problem domain exclusively on the basis of the training data. Thus, beginning of authors' research concerning the neural network application in loaded microwave cavity modeling was based on MLP neural model [13]. Such model was trained by using TRM as experimentally verified and therefore referent approach for this type of problems [3].

In order to achieve the acceptable accuracy in the process of loaded cavity resonant frequencies determination by using MLP model, a large set of data was needed for training purposes leading to very difficult and time-consuming process [14]. One way to decrease the number of training samples and keep the required accuracy is to use a knowledge based neural (KBN) network [5, 14]. Such neural network allows for incorporation of already known functional dependences about modeling problem into the transfer function of some KBN neurons. In reference [15], a KBN model was proposed for loaded cavity modeling providing the significantly better accuracy than MLP model using fewer training samples. Presented model was intended to solve only the particular case of cavity loaded with dielectric slab placed at the cavity bottom and therefore it incorporated an existing partial knowledge about resonant frequency behavior of such loaded cavity. This KBN model was successfully validated by experimental and referent TRM results.

In a number of practical microwave heating and drying applications, dielectric slab can have changeable elevation from the cavity bottom resulting in more complex configuration of microwave applicators. Arbitrary raised dielectric slab represents a generalization of the case when dielectric material is placed at the cavity bottom. Such general cavity load form is very difficult to solve using KBN network architecture presented in [15], because incorporated partial knowledge of resonant frequency behavior does not include explicitly the influence of dielectric slab elevation. One way to describe arbitrary

raised dielectric slab influence on cavity resonant frequency and still keep the advantages of neural network modeling is to modify empirical approach based an approximate model [4] and to combine it with appropriate neural network. In this paper, empirical approach is modified in terms that linear approximation is used to account for dependence of resonant frequency curves on arbitrary elevation of cavity load. Such approximate model provides a rough resonant frequency solution, which can be further refined using MLP network forming a hybrid empirical-neural (HEN) model. This hybrid model is able to provide accurate modeling when training set is too small and when acceptable accuracy can not be achieved using classical MLP model alone. In addition, previously analyzed case of load in the form of dielectric slab located on the cavity bottom can be easily treated by new model as a special case of more general raised dielectric load form. HEN model accuracy and efficiency are illustrated through comparison with experimental and referent TRM results obtained for the case of resonant frequency determination of the TM_{112} mode in a cylindrical metallic cavity with circular cross-section.

2. KNOWLEDGE ABOUT LOADED CAVITY RESONANT FREQUENCY

Conducted research presented in [3] has shown that the resonant frequency f_r of excited TM/TE_{mnp} mode in a cylindrical metallic cavity loaded by homogeneous dielectric slab elevated from the cavity bottom (Fig. 1) can be expressed as a following function:

$$f_r = f(t_h, \varepsilon_r, e_h) \tag{1}$$

where: ε_r, is a relative dielectric permittivity, t_h is a filling factor ($t_h = t/h$, where $t$is thickness of dielectric slab and h is height of the cavity) and eh is an elevation factor e_h ($e_h = e/h$, where e is the elevation of dielectric slab from the cavity bottom).

Using short-circuit boundary (electric wall) in a interface plane between dielectric slab and air, for the the special case when $e_h = 0$, the following equations are derived from the condition of resonance applied separately in air and dielectric part of the cavity:

$$h - t = \ell \cdot \frac{\lambda_{t0}}{2} \tag{2}$$

$$t = k \cdot \frac{\lambda_t}{2} \tag{3}$$

where λ_{t0} is a wavelength of waveguide filled with air, λ_t is a wavelength of waveguide filled with dielectric material and with the same cross-

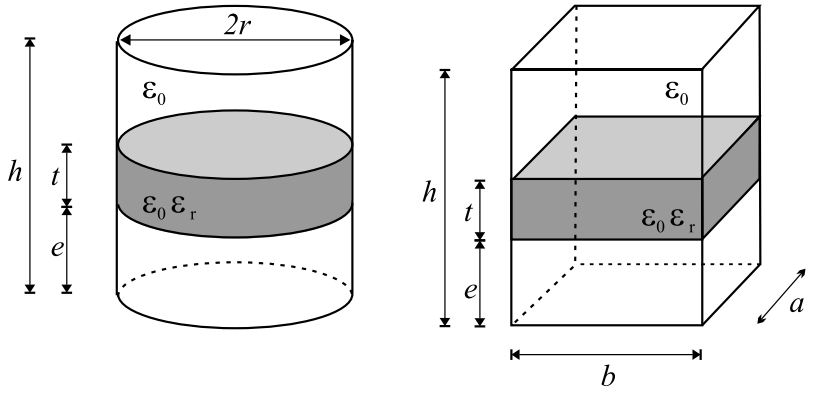

Figure 1. Microwave cylindrical metallic cavity with circular and rectangular cross-section loaded by dielectric slab of thickness t and elevation e from the cavity bottom.

section as considered cavity, while integers l and k are the number of half waves of standing wave for electric field in corresponding part of the cavity. From the expression for phase constant:

$$\beta^2 = \left(\frac{2\pi}{\lambda_t}\right)^2 = (2\pi f)^2 \varepsilon\mu - k_c^2 \tag{4}$$

frequency f can be expressed as

$$f^2 = \left(\frac{c}{\sqrt{\varepsilon_r}}\frac{1}{\lambda_t}\right)^2 + \left(\frac{f_{c0}}{\sqrt{\varepsilon_r}}\right)^2 \tag{5}$$

where $f_{c0} = ck_c/(2\pi)$ represents the cutoff frequency of a waveguide with the same cross-section as cavity and filled with air, while k_c is a constant that depends on mode of oscillation and waveguide cross-section shape and dimensions [2].

From the Eqs. (2), (3) and (5), the appropriate expressions for resonant frequency calculation in air and dielectric part of cavity can be easily derived as a function of filling factor t_h:

$$f_{r(\ell)}^{(A)}(t_h) = \sqrt{\left(\ell \cdot \frac{f_0}{1-t_h}\right)^2 + f_{c0}^2} \quad \ell = \begin{cases} 0,1,2,\ldots & \text{for TM}_{mnp} \text{ modes} \\ 1,2,3,\ldots & \text{for TE}_{mnp} \text{ modes} \end{cases} \tag{6}$$

$$f_{r(k)}^{(D)}(t_h, \varepsilon_r) = \sqrt{\left(k \cdot \frac{f_0}{\sqrt{\varepsilon_r}}\frac{1}{t_h}\right)^2 + \left(\frac{f_{c0}}{\sqrt{\varepsilon_r}}\right)^2} \quad k = 1,2,3,\ldots \tag{7}$$

where $f_0 = c/(2h)$.

Applying open-circuit boundary (magnetic wall) in the interface plane between dielectric and air, for the the special case when $e_h = 0$, the following equations are derived from anti-resonant condition applied separately in air and dielectric part of the cavity:

$$h - t = (2\ell - 1) \cdot \frac{\lambda_{t0}}{4} \tag{8}$$

$$t = (2k - 1) \cdot \frac{\lambda_t}{4} \tag{9}$$

Similarly, from the Eqs. (5), (8) and (9), the appropriate expressions for anti-resonant frequency calculation in air and dielectric part of the cavity can be found as:

$$f_a^{(A)}(t_h) = \sqrt{\left(\frac{2\ell - 1}{2} \cdot \frac{f_0}{1 - t/h}\right)^2 + f_{c0}^2} \quad l = 1, 2, 3, \ldots \tag{10}$$

$$f_a^{(D)}(t_h, \varepsilon_r) = \sqrt{\left(\frac{2k - 1}{2} \cdot \frac{f_0}{\sqrt{\varepsilon_r}} \cdot \frac{1}{t/h}\right)^2 + \left(\frac{f_{c0}}{\sqrt{\varepsilon_r}}\right)^2} \quad k = 1, 2, 3, \ldots \tag{11}$$

Detailed semi-empirical analysis of cylindrical metallic cavities loaded with raised dielectric slab [3] has shown that resonant frequency curves, for considered TM/TE$_{mnp}$ mode excited in such cavities, independently of the elevation factor value, are passing through characteristic points $\mathrm{RR}_k^l(\varepsilon_r)$ (Fig. 2a), already identify in [15] as a crossing point of k-th resonant curve in dielectric part of the cavity (RD curve) and l-th resonant curve in air part of the cavity (RA curve). In addition, for the special case of cavity load position (cavity load placed at the cavity bottom, $e_k = 0$), characteristic points $\mathrm{AA}_k^l(\varepsilon_r)$ (Fig. 2b), as a crossing point of k-th anti-resonant curve in dielectric part of the cavity (ARD curve) and l-th anti-resonant curve in air part of the cavity (ARA curve) are also of interest for resonant frequency curves determination. The characteristic points are easily found from Eqs. (6), (7), (10) and (11) for known relative permittivity ε_r.

As it can be seen from Fig. 2(a), with the increase of filling factor t_h, resonant frequency curves are passing through characteristic points with the following order: F_0^A, $\mathrm{RR}_1^{(p-1)}$, $\mathrm{RR}_2^{(p-2)}$, ..., $\mathrm{RR}_p^{min(l)}$, where F_0^A is the characteristic point determined by the resonant frequency of an empty cavity. In these points, resonant frequencies of considered oscillated mode, for a given value of dielectric permittivity, are the same irrespectively to the value of elevation factor. In the areas

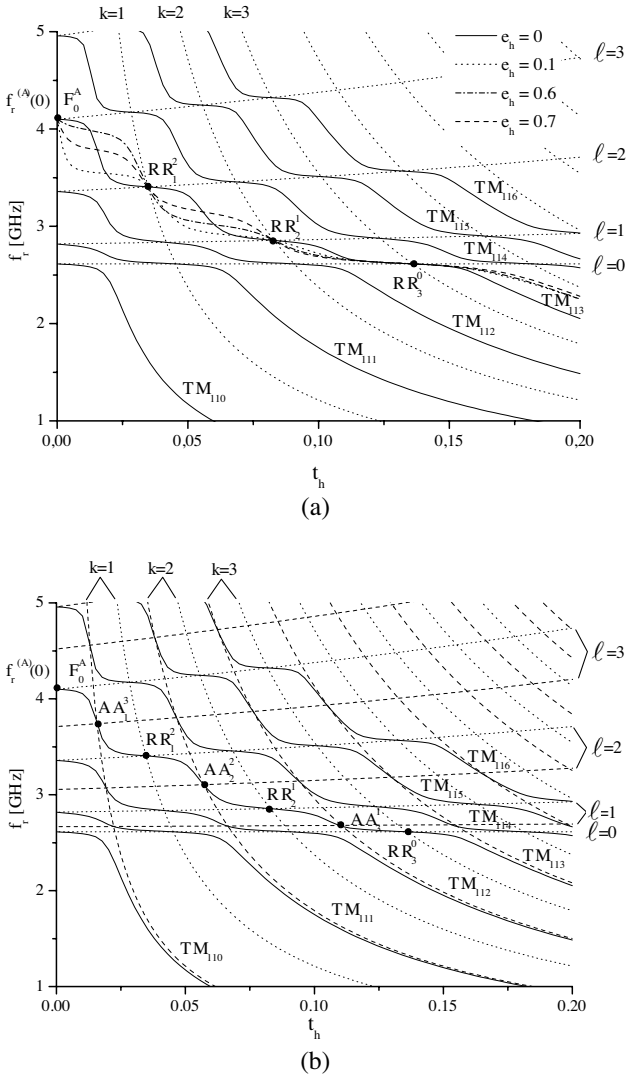

Figure 2. Family of the resonant frequencies for TM_{11p} mod obtained using TRM for the cylindrical metallic cavity with circular cross-section ($r = 7\,\text{cm}$ and $h = 14.24$) loaded with dielectric slab of relative permittivity $\varepsilon_r = 80$ for: (a) different elevation factors e_h, (b) for elevation factor $e_h = 0$. $\cdots$ resonant curves monotonous increasing in air part (RA curves) and monotonous decreasing in dielectric part of the cavity (RD curves). - - - anti-resonant curves monotonous increasing in air part (ARA curves) and monotonous decreasing in dielectric part of the cavity (ARD curves).

between characteristic points $\mathrm{RR}_k^l(\varepsilon_r)$, there are small deviations of resonant frequencies in comparison with the whole range of their changes. Thus, for each pair of characteristic points RR_k^{λ} i $\mathrm{RR}_{k+1}^{\ell-1}$ and their corresponding filling factors $(t_{hp})^{\varepsilon_r}_{\mathrm{RR}_k^{\ell}}$ and $(t_{hp})^{\varepsilon_r}_{\mathrm{RR}_{k+1}^{\ell-1}}$, linear function passing through these points could be used for a rough approximation of resonant frequency curve in $[(t_{hp})^{\varepsilon_r}_{\mathrm{RR}_k^{\ell}},\ (t_{hp})^{\varepsilon_r}_{\mathrm{RR}_{k+1}^{\ell-1}}]$ segment.

In the area where filling factor is greater than the filling factor corresponding to the last characteristic point in series ($t_h > (t_{hp})^{\varepsilon_r}_{\mathrm{RR}_p^{\min(\ell)}}$), point A' on anti-resonant curve given by Eq. (11) for $k = p + 1$, having the same value of resonant frequency as the last characteristic point $\mathrm{RR}_p^{\min(l)}$, can be noticed. As an illustration, location of point A' for mode TM_{113} ($p = 3$) is shown in Fig. 3. Value of filling factor corresponding to the point A' is:

$$t'_h = (t_{hp})^{\varepsilon_r}_{A'} = \frac{2p+1}{2} \cdot \frac{f_0}{\sqrt{\varepsilon_r \cdot \left[(f_{rp})^{\varepsilon_r}_{\mathrm{RR}_p^{\min(\ell)}}\right]^2 - f_{c0}^2}} \tag{12}$$

On the same anti-resonant curve, an additional point A can be defined. The filling factor corresponding to this point is:

$$t_h^A = (t_{hp})^{\varepsilon_r}_{A} = t'_h + \left(t'_h - (t_{hp})^{\varepsilon_r}_{\mathrm{RR}_p^{\min(\ell)}}\right) \tag{13}$$

while the value of resonant frequency is:

$$(f_r)^{\varepsilon_r}_{A} = f^{(D)}_{a(p+1)}\left(t_h^A, \varepsilon_r\right) = \sqrt{\left(\frac{2p+1}{2} \cdot \frac{f_0}{\sqrt{\varepsilon_r}} \cdot \frac{1}{t_h^A}\right)^2 + \left(\frac{f_{c0}}{\sqrt{\varepsilon_r}}\right)^2} \tag{14}$$

Point A determines the segment $[(t_{hp})^{\varepsilon_r}_{\mathrm{RR}_p^{\min(\ell)}},\ (t_{hp})^{\varepsilon_r}_{A}]$ in which the value of resonant frequency is approximated by linear function passing through the last characteristic point and point A. For the filling factor values $t_h > (t_{hp})^{\varepsilon_r}_{A}$, resonant frequency is approximated by anti-resonant curve given by Eq. (11) for $k = p + 1$. Therefore, resonant frequency curves of cylindrical metallic cavities loaded with raised dielectric slab can be roughly described with the following general function notation (so-called approximate model):

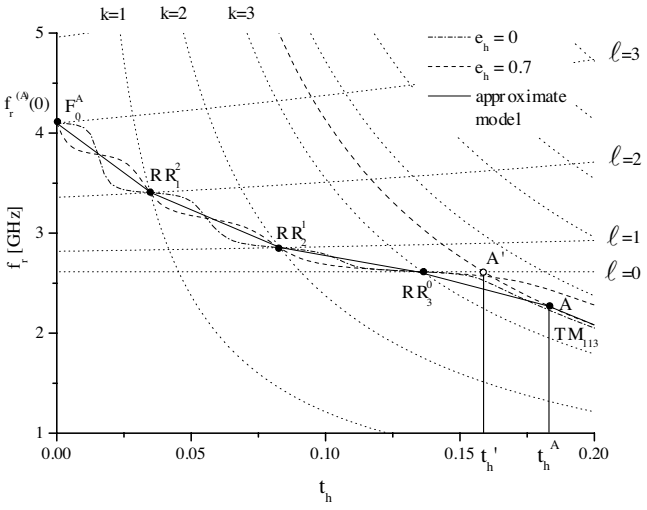

Figure 3. Resonant frequencies of TM_{113} mode, for the cylindrical metallic cavity with circular cross-section ($r = 7\,\text{cm}$ and $h = 14.24$) loaded with dielectric slab of relative permittivity $\varepsilon_r = 80$, versus filling factor t_h obtained by TRM for two different elevation factor values (dotted line) and by linear approximation model (solid line).

$$
f_r^{AP}(t_h,\varepsilon_r) =
\begin{cases}
\dfrac{(f_{rp})^{\varepsilon_r}_{\mathrm{RR}_1^{(p-1)}} - f^{(A)}_{r(p)}}{(t_{hp})^{\varepsilon_r}_{\mathrm{RR}_1^{(p-1)}}} \cdot t_h + f^{(A)}_{r(p)}, & 0 \le t_h < (t_{hp})^{\varepsilon_r}_{\mathrm{RR}_1^{(p-1)}} \\
\dfrac{(f_{rp})^{\varepsilon_r}_{\mathrm{RR}_2^{(p-2)}} - (f_{rp})^{\varepsilon_r}_{\mathrm{RR}_1^{(p-1)}}}{(t_{hp})^{\varepsilon_r}_{\mathrm{RR}_2^{(p-2)}} - (t_{hp})^{\varepsilon_r}_{\mathrm{RR}_1^{(p-1)}}} & \\
\cdot\left(t_h - (t_{hp})^{\varepsilon_r}_{\mathrm{RR}_1^{(p-1)}}\right) + (f_{rp})^{\varepsilon_r}_{\mathrm{RR}_1^{(p-1)}} & , \quad (t_{hp})^{\varepsilon_r}_{\mathrm{RR}_1^{(p-1)}} \le t_h < (t_{hp})^{\varepsilon_r}_{\mathrm{RR}_2^{(p-2)}} \\
\vdots & \\
\dfrac{(f_{rp})^{\varepsilon_r}_{A} - (f_{rp})^{\varepsilon_r}_{\mathrm{RR}_p^{\min(l)}}}{(t_{hp})^{\varepsilon_r}_{A} - (t_{hp})^{\varepsilon_r}_{\mathrm{RR}_p^{\min(l)}}} & \\
\cdot\left(t_h - (t_{hp})^{\varepsilon_r}_{\mathrm{RR}_p^{\min(l)}}\right) + (f_{rp})^{\varepsilon_r}_{\mathrm{RR}_p^{\min(l)}} & , \quad (t_{hp})^{\varepsilon_r}_{\mathrm{RR}_p^{\min(l)}} \le t_h < (t_{hp})^{\varepsilon_r}_{A} \\
f^{(D)}_{a(p+1)}(t_h,\varepsilon_r), & (t_{hp})^{\varepsilon_r}_{A} \le t_h < 0.2
\end{cases}
\tag{15}
$$

Fact that $\mathrm{RR}_k^l(\varepsilon_r)$ and $\mathrm{AA}_k^l(\varepsilon_r)$ points describe to some extent the behavior of resonant frequency curves (mode tuning behavior) for different values of elevation factor and that they are determined directly by resonant frequency functions in air and dielectric part of the cavity, given in analytical form, allows that approximate model provides rough but quick solution of loaded cavity resonant frequency.

3. HYBRID EMPIRICAL-NEURAL MODEL OF LOADED CAVITY

Architecture of the proposed hybrid empirical-neural model for resonant frequency determination of the cylindrical metallic cavity loaded with arbitrary raised dielectric slab is presented in Fig. 4. It is based on so-called PKI (Prior Knowledge Input) approach in which empirical model with corresponding connection to the neural network

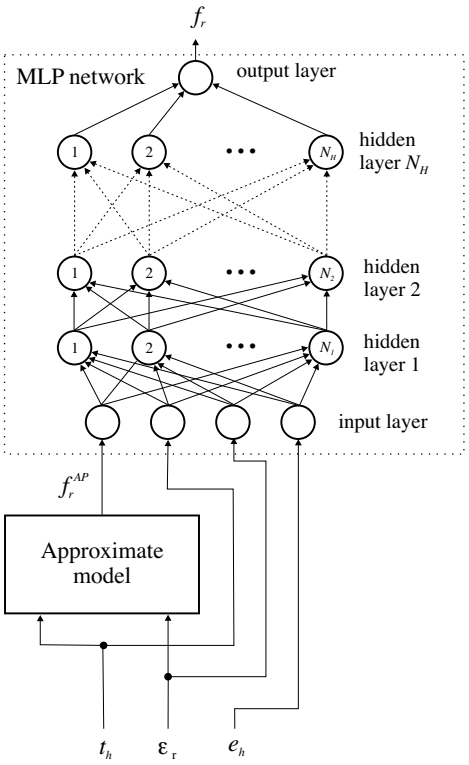

Figure 4. Architecture of proposed hybrid empirical-neural (HEN) model of the cylindrical metallic cavity loaded with arbitrary raised dielectric slab.

provides higher generalization of the network [5]. In this paper, this is achieved by presenting extra information about the problem at the input of the neural network.

Approximate model, defined in Section 2, is used as empirical model in this hybrid structure. Input in such model is represented by vector $\mathbf{x^{AP}} = [t_h \ \varepsilon_r]^T$ while its output is approximate value of resonant frequency f_r^{AP}. Approximate model determines the resonant frequency f_r^{AP} in three steps (Fig. 5). In the first step, resonant and anti-resonant frequency curves in air and dielectric part of the cavity are implemented in analytical form for TM/TE$_{mnp}$ modes and for considered cavity; Eqs. (6), (7), (10), and (11). In the second step, based on previously implemented resonant and anti-resonant modes, the co-ordinates of characteristic points are numerically determined for given mode and given relative permittivity of dielectric material. Finally, for given filling factor the value of resonant frequency between the characteristic points is approximated by linear function described in Eq. (15).

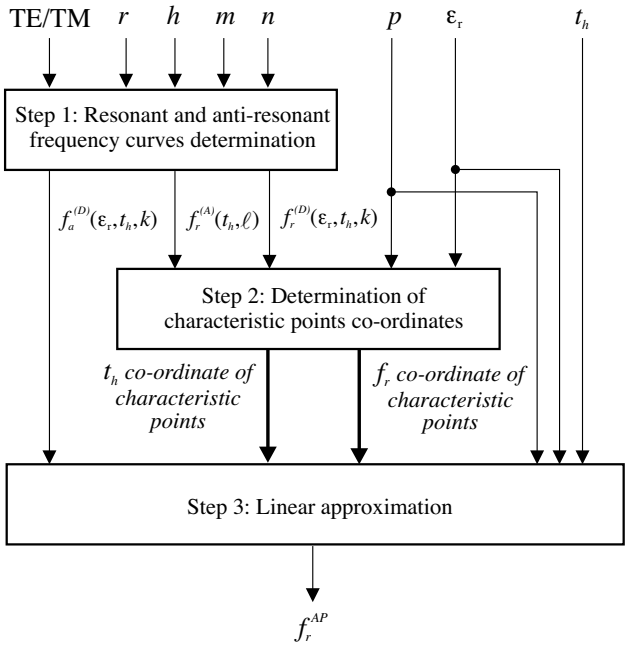

Figure 5. Flow chart of data processing in approximated model.

MLP network is used as a neural network of proposed HEN model (Fig. 4). Its task is, based on resonant frequency information obtained

from approximate model, f_r^{AP}, and based on input parameters values, to determine accurately the resonant frequencies of cylindrical metallic cavity loaded with arbitrary raised dielectric slab. It consists of neurons grouped into the following layers: an input layer, an output layer and one or more hidden layers of sigmoid neurons. The buffered input layer contains four neurons corresponding to f_r^{AP}, t_h, ε_r and e_h, ($\mathbf{x} = [f_r^{AP}\ t_h\ \varepsilon_r\ e_h]^T$), while output layer contains one linear neuron which correspond to f_r. The number of neurons in the hidden layers can be variable. Among neurons in the same layer, there are no connections. Inputs of each neuron from l-th hidden layers are outputs of all neurons from $(l-1)$-th hidden layer. Vector of l-th hidden layer outputs of MLP network is:

$$\mathbf{y}_l = F(\mathbf{w}_l \mathbf{y}_{l-1} + \mathbf{b}_l) \tag{16}$$

where: $\mathbf{y}_l$ is a $N_l \times 1$ vector of $l-$th hidden layer outputs, $\mathbf{y}_{l-1}$ is a $N_{l-1} \times 1$ vector of $(l-1)$-th hidden layer outputs, $\mathbf{w}_l$ is a $N_l \times N_{l-1}$ connection weight matrix among $(l-1)$-th and l-th hidden layer neurons and $\mathbf{b}_l$ is a vector containing biases of l-th hidden layer neurons. In the above notation $\mathbf{y}_0$ represents outputs of the buffered input layer $\mathbf{y}_0 = \mathbf{x} = [f_r^{AP}\ t_h\ \varepsilon_r\ e_h]^T$. F is the transfer function of hidden layer neurons and it is a hyperbolic tangent sigmoid transfer function

$$F(u) = \frac{e^u - e^{-u}}{e^u + e^{-u}} \tag{17}$$

All neurons from the last hidden layer H are connected with the neuron of the output layer. Since the transfer function of output layer is linear, the output of the KBN network is

$$f_r = \mathbf{w}_o \mathbf{y}_H \tag{18}$$

where $\mathbf{w}_o$ is a $1 \times N_H$ connection weight matrix among the H-th hidden layer neurons and output layer neuron. Based on this, MLP network in HEN model can be described with the following general function notation

$$f_r = f(\mathbf{x}, W) \tag{19}$$

where $\mathbf{x}$ represents vector of input variables in MLP part of HEN model, $\mathbf{x} = [f_r^{AP}\ t_h\ \varepsilon_r\ e_h]^T$ and $\boldsymbol{W}$ is weight matrix of MLP network, $W = \{\mathbf{w}_1, \ldots, \mathbf{w}_H, \mathbf{w}_o, \mathbf{b}_1, \ldots, \mathbf{b}_H\}$. General symbol of HEN model is HEN$H - N_1$-...-N_i-...-N_H where Hrepresents the total number of hidden layers in MLP network while N_i is the number of neurons in the $i-$th MLP hidden layer.

Important step in HEN model developing is training of its neural network part. For presented architecture, neural network

learning of relationship (1) uses a set of training data $S = \left\{(\mathbf{x'}_s, f'^d_{rs}),\ s = 1, 2, \ldots, N_S\right\}$ where $\mathbf{x}'_s$ is a vector of input parameters that includes, besides dielectric permittivity and filling factor, the resonant frequency obtained from empirical part of the model and the elevation factor ($\mathbf{x'}_s = [f_r^{AP\prime}\ t'_h\ \varepsilon'_r\ e_h]^T$), f'^d_{rs} is desired network output for $\mathbf{x'}_s$ at its inputs and N_S is a total number of data samples. Training goal is to achieve the total error $E(W)$, between the desired outputs and the actual outputs f'_{rs} from MLP network, lower than the prescribed value E_c by adjusting matrix parameters W.

$$E_c > E(W) = \frac{1}{2}\sum_{s=1}^{N_S}\left(f'^d_{rs} - f'_{rs}\right)^2 \tag{20}$$

As MLP network belongs to non-recurrent neural structures, gradient-based algorithms, such as Quasi-Newton's or Levenberg Marquardts algorithms [5, 11], can be used for network parameters adjustment.

In order to reduce additionally the training set and to increase the modeling efficiency, a modification of non-uniform distribution of the training samples, presented in [15], is used. This is done according to the behavior of resonant frequencies in t_h-ε_r space. For given ε_r and e_h, the values which correspond to the characteristic points RR of the modeled TM/TE$_{mnp}$ mode, to three equidistant added points between them, as well as to the boundary points (for $t_h = 0$ and $t_h = 0.2$) are used for input parameter t_h

$$I_{t_h} = \left\{0, \frac{(t_h)_{\mathrm{RR}_1^{P-1}}}{4}, \frac{(t_h)_{\mathrm{RR}_1^{P-1}}}{2}, \frac{3\cdot(t_h)_{\mathrm{RR}_1^{P-1}}}{4}, (t_h)_{\mathrm{RR}_1^{P-1}}, \ldots, 0.2\right\} \tag{21}$$

Values of ε_r are generated in the following way

$$\varepsilon_{ri} = 1 + i^2, \quad i = 1, 2, \ldots, 9 \tag{22}$$

The values for input parameters e_h, are

$$I_{e_h} = \{0, 0.2, 0.4, 0.6, 0.8\} \tag{23}$$

For each combination of the input parameters from the set

$$X_P = \bigcup_{i=1}^{9} I_{t_h} \times \{\varepsilon_{ri}\} \times I_{e_h} \tag{24}$$

the corresponding resonant frequency is computed by TRM and in that way the samples for the training set are provided. After the

training process is finished, adjustable network parameters are not changed any more during the model exploitation. Trained HEN model has a generalization capability, i.e., to provide a fast response for arbitrary vector from the input space without any additional change of its structure or its parameters.

Testing process of trained models is conducted next. Purpose of HEN model testing is to determine the training success, i.e. to estimate the model accuracy in its real applications. For model testing, a data set of the same format as training set (arrange set of 5 elements which consists of testing vales of input parameters not used during the training and value of expected resonant frequency at the model output for these input parameters) is used. Based on HEN model values of resonant frequency at its output, obtained for all input parameters values from test set, and expected (referent) resonant frequency values for the same input parameters, statistical analysis of error at HEN model output is done. This analysis includes the calculation of average test error (ATE [%]), worst-case error (WCE [%]), and Pearson Product-Moment correlation coefficient (r^{PPM}) [5, 15].

4. MODELING EXAMPLE

In this section, the proposed HEN approach is applied to calculate TM_{112} mode resonant frequencies of the experimental cylindrical metallic cavity with circular cross-section with dimensions $r = 7\,\text{cm}$ and $h = 14.24$ (Fig. 6(a) and Fig. 6(b)). Input parameters and their ranges are given in Table 1. For the training purposes, a set of non-uniform samples, whose distribution is described in the previous section, is generated by using TRM (82 samples per elevation factor giving in total 410 samples). In order to obtain a model as good as possible, training of various HENH-N_1-...-N_i-...-N_H networks where $1 \leq H \leq 3$ and $1 \leq N_i \leq 30$, is done using the same training set P. In addition, for the purpose of comparing HEN models with classical MLP models, the same sample set is used for classical MLP models training. *Levenberg* Marquardt's training algorithm with prescribed error value $E_{ck} = 10^{-4}$ is chosen.

Table 1. Ranges of input and output parameters of the neural model.

I/O parameter	t_h	ε_r	e_h	f_r
I/O type	input	input	input	output
Range	0–0.2	2–82	0–0.8	0–10 GHz

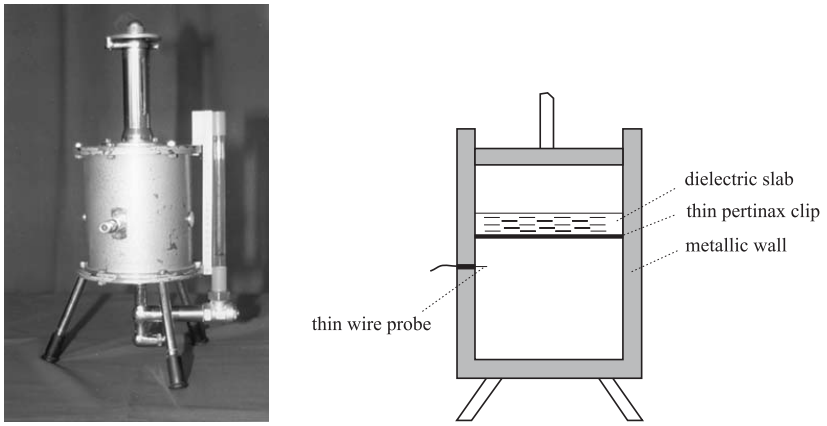

Figure 6. (a) Experimental cylindrical metallic cavity with circular cross-section, (b) dielectric slab elevated from the cavity bottom by using thin pertinax clip.

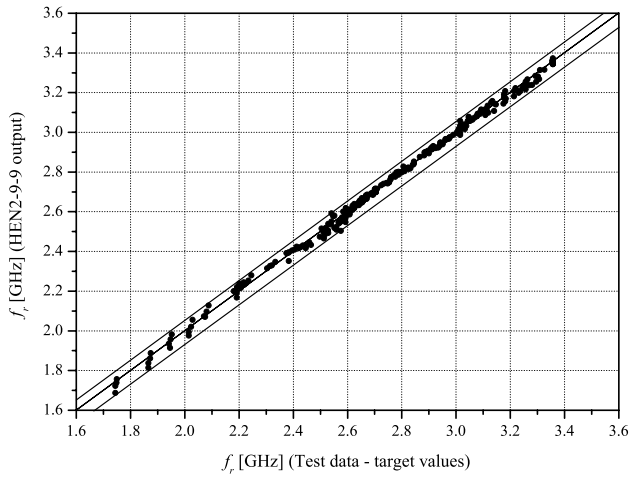

Figure 7. Scattering diagram for HEN2-9-9 model.

Testing of both HEN and classical MLP models, for testing data set (320 uniformly distributed samples) not used in their training process, is done. The testing results for eight HEN models and for eight MLP models with the highest r^{PPM} correlation coefficient are shown in Table 2 and Table 3, respectively. It can be seen that the HEN models show significantly lower average testing errors (ATE and WCE) and

higher r^{PPM} correlation coefficients than classical MLP models. For HEN and MLP model with the highest r^{PPM} correlation factor for a given testing set (HEN2-9-9 and MLP2-12-12), appropriate scattering diagrams (Fig. 7 and Fig. 8) show that HEN model has significantly less deviation of output parameters from their expected values than classical MLP model.

Table 2. Testing results for eight HEN models.

HEN model	Worst case error [%]	Average error [%]	r^{PPM}
HEN2-9-9	4.41	0.76	0.9990
HEN2-8-8	4.74	0.76	0.9990
HEN2-12-11	5.03	0.73	0.9990
HEN2-10-8	4.38	0.77	0.9990
HEN2-14-11	4.78	0.78	0.9988
HEN2-14-12	4.09	0.80	0.9988
HEN2-10-4	4.04	0.80	0.9987
HEN2-15-9	6.52	0.82	0.9986

Table 3. Testing results for eight MLP models.

MLP model	Worst case error [%]	Average error [%]	r^{PPM}
MLP2-12-12	8.83	1.41	0.9970
MLP2-12-8	12.59	1.30	0.9963
MLP2-20-20	8.65	1.54	0.9961
MLP2-20-15	9.87	1.54	0.9958
MLP2-14-11	18.56	1.23	0.9965
MLP2-22-22	10.37	1.60	0.9959
MLP2-9-9	11.06	1.58	0.9958
MLP2-18-16	12.32	1.81	0.9954

The same models are selected for the TM_{112} mode simulation: HEN model (HEN2-9-9) and classical MLP model (MLP2-12-12). The resonant frequency values obtained by these two models are compared with the measured data, for the case when water slab is raised from the cavity bottom at height $e = 0.65h$ (Fig. 9). Elevation of water is achieved by thin pertinax clip of thickness 0.9 mm and low permittivity in considered frequency range, fixed by silicone glue to the cavity walls in order to achieve waterproofing below clip (Fig. 6(b)). Such clip parameters provide insignificant influence to the resonant

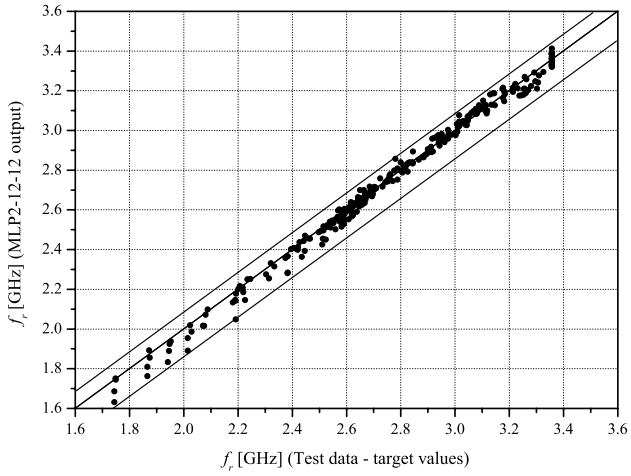

Figure 8. Scattering diagram for MLP2-12-12 model.

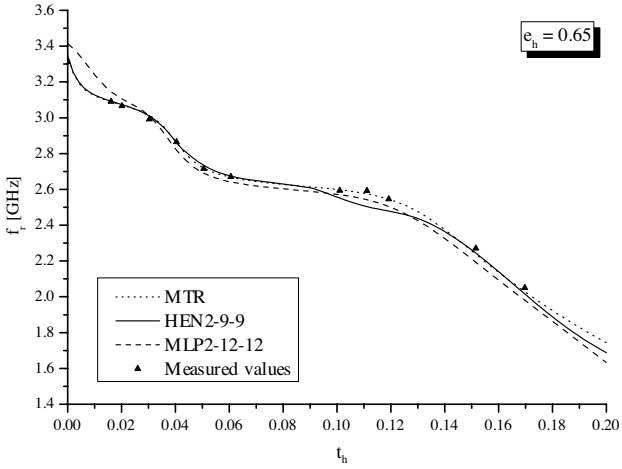

Figure 9. Resonant frequency of TM_{112} mode obtained by using KBN-MLP model, MLP model, TRM and measurement vs. filling factor for the case of water dielectric slab with elevation factor $e_h = 0.65$.

frequency measurements. Measurement of the resonant frequencies was performed using a HP8753C network analyzer in the frequency range from 1 to 4 GHz at ambient temperature equals 20°C (a detailed description of used experimental set-up can be found in [16]). The

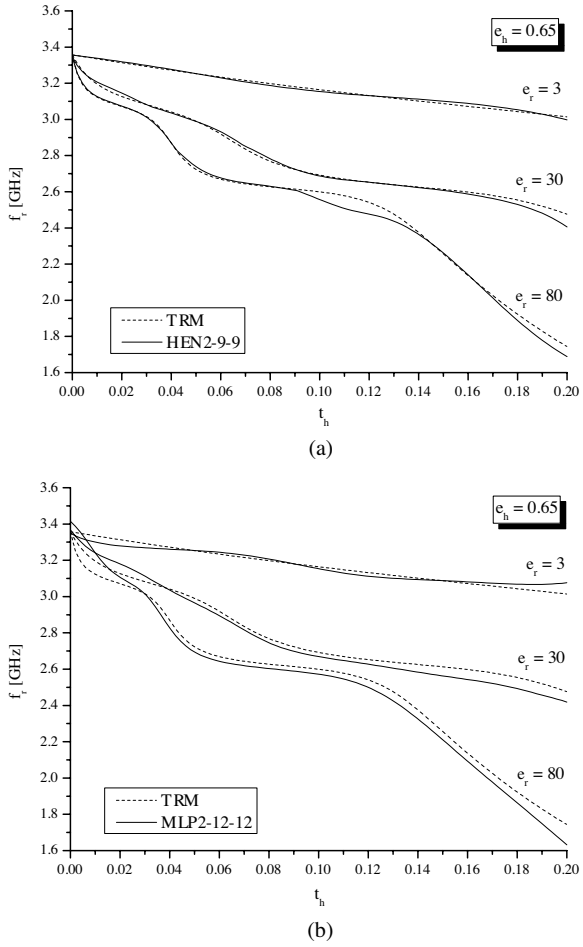

Figure 10. Resonant frequency of TM_{112} mode obtained by using (a) HEN model and TRM, (b) MLP model and TRM (referent curve) vs. filling factor for different values of relative dielectric permittivity (3, 30, 80) and elevation factor $e_h = 0.65$.

analysis of the presented results shows that simulated values obtained using HEN2-9-9 model are closer to the measured values than the values obtained using MLP2-11-11 model (Fig. 9).

In addition, TRM results follow experimental results confirming the approach of using TRM for training and validation purposes of developed neural models. Therefore, the values of resonant frequency for elevation factor $e_h = 0.65$ (Fig. 10(a) and Fig. 10(b)) and $e_h = 0.45$

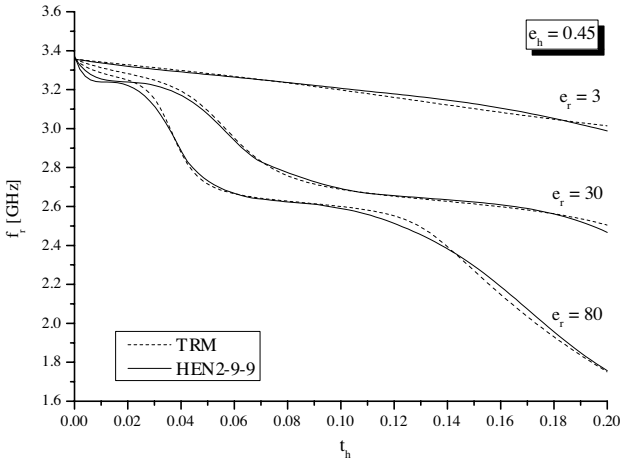

Figure 11. Resonant frequency of TM_{112} mode obtained by using a) HEN model and TRM, b) MLP model and TRM (referent curve) vs. filling factor for different values of relative dielectric permittivity (3, 30, 80) and elevation factor e_h=0.45.

(Fig. 11(a) and Fig. 11(b)) and three values of relative permittivity ε_r (3,30,80) obtained by these two models are compared with the referent curves obtained using the TRM. Again, the same conclusion can be derived that HEN2-9-9 model provides better accuracy than MLP2-11-11 model.

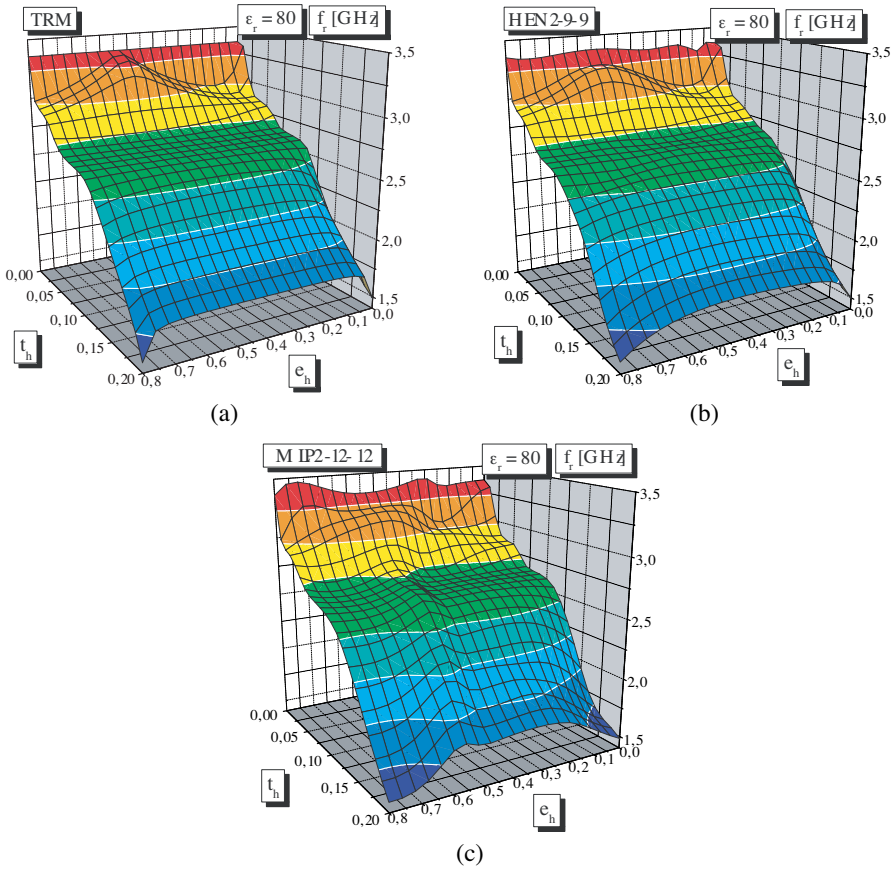

Figure 12. Resonant frequency of TM_{112} mode vs. cavity filling factor and elevation factor obtained by using (a) TRM, (b) HEN model, and (c) MLP model.

Further, a three-dimensional (3D) presentation of the resonant frequency dependence versus the cavity filling factor t_h and elevation factor e_h obtained by these models is presented in Fig. 12(b) (HEN2-9-9) and in Fig. 10(c) (MLP2-11-11). Comparing these 3D plots with the referent surface obtained using TRM (shown in Fig. 10(a), it can be seen that the surface obtained by HEN model is more similar to the referent surface than the surface obtained by MLP model. For 3D plot generating in 10000 points per area both models take 3–5 sec, while transverse resonance method takes about 20 hours to run on Pentium III 1.1 GHz–128 MB RAM hardware platform.

5. CONCLUSION

Neural network models represents an accurate and faster alternative to EM models, based on numerical methods (such as transverse resonant method), for loaded microwave cavity modeling. However, classical neural network approach based on MLP network needs a large number of training samples to provide required model accuracy. Increase of neural network modeling efficiency can be achieved by incorporating an existing partial knowledge from problem domain into the model architecture. First approach of knowledge incorporation is to use the KBN network which at the moment can be applied only to particular case of dielectric slab placed at the cavity bottom. However, in real applications of microwave heating and drying, more general cavity load case in the form of arbitrary raised dielectric slab can be often found. Good solution for such loaded cavity modeling offers the second knowledge incorporation approach, based on realization of the hybrid empirical-neural network, presented in this paper. HEN model provides the satisfied accuracy for significantly smaller number of training samples than MLP network or in the case of fewer training samples provides significantly better accuracy than MLP network on the same training set. Such capabilities of developed HEN model are illustrated on the example of resonant frequency determination of the TM_{112} mode in an experimental cylindrical metallic cavity with circular cross-section.

REFERENCES

1. Chan, T. V. C. T. and H. C. Reader, *Understanding Microwave Heating Cavities*, Artech House, 2000.
2. Balanis, C. A., *Advanced Engineering Electromagnetics*, John Wiley & Sons, Inc., New York, 1989.
3. Milovanović, B., S. Ivković, D. Djordjević, and N. Dončov, "The loading effect analysis of the cylindrical metallic cavities with various cross-sections," *Journal of Microwave Power and Electromagnetic Energy*, Vol. 33, No. 1, 49–55, 1998.
4. Milovanović, B., S. Ivković, and A. Atanasković, "Approximate resonant frequency determination of the cylindrical metallic cavities loaded by lossy dielectric slab," *Journal of Microwave Power and Electromagnetic Energy*, Vol. 33, No. 1, 49–55, 1999.
5. Zhang, Q. J. and K. C. Gupta, *Neural Networks for RF and Microwave Design*, Artech House, 2000.
6. Guney, K., S. Sagiroglu, and M. Erler, "Comparison of neural

networks for resonant frequency computation of electrically thin and thick rectangular microstrip antennas," *Journal of Electromagnetic Wave and Applications*, Vol. 15, 1121–1145, 2001.

7. Mohamed, M. D. A., E. A. Soliman, and M. A. El-Gamal, "Optimization and characterization of electromagnetically coupled patch antennas using RBF neural networks," *Journal of Electromagnetic Wave and Applications*, Vol. 20, 1101–1114, 2006.
8. Guney, K., C. Yildiz, S. Kaya, and M. Turkmen, "Artificial neural networks for calculating the characteristic impedance of airsuspended trapezoidal and rectangular-shaped microshield lines," *Journal of Electromagnetic Wave and Applications*, Vol. 20, 1161–1174, 2006.
9. Ayestarán, R. G., F. Las-Heras, and J. A. Martínez, "Nonuniform-antenna array synthesis using neural networks," *Journal of Electromagnetic Waves and Applications*, Vol. 21, 1001–1011, 2007.
10. Kizilay, A. and S. Makal, "A neural network solution for identification and classification of cylindrical targets above perfectly conducting flat surfaces," *Journal of Electromagnetic Waves and Applications*, Vol. 21, 2147–2156, 2007.
11. Yildiz, C., K. Guney, M. Turkmen, and S. Kaya, "Neural models for coplanar strip line synthesis," *Progress In Electromagnetics Research*, PIER 69, 127–144, 2007.
12. Haykin, S., *Neural Networks*, IEEE, New York, 1994.
13. Milovanović, B., Z. Stanković, and S. Ivković, "Modelling of the cylindrical metallic cavity with circular cross-section using neural networks," *Proceedings of IEEE 10th Mediterranean Electrotechnical Conference — MELECON'2000*, Vol. 2, 449–452, Cyprus, 2000.
14. Wang, F. and Q. J. Zhang, "Knowledge based neural networks for microwave design," *IEEE Trans Microwave Theory and Tech.*, Vol. 45, No. 12, 2333–2343, 1997.
15. Stanković, Z. and B. Milovanović, "Microwave loaded cylindrical cavity modeling using knowledge based neural network," *Microwave Opt. Technol. Lett.*, Vol. 46, No. 6, 585–588, 2005.
16. Jokoviić, J., B. Milovanović, and N. Dončov, "TLM analysis of cylindrical metallic cavity excited with a real feed probe," *Int. Journal RF Microwave Computer-Aided Engineering*, Vol. 16, No. 4, 346–354, 2006.